Photochemical & Photobiological Sciences

PAPER

View Article Online
View Journal | View Issue

Cite this: *Photochem. Photobiol. Sci.*, 2015, **14**, 329

Singlet oxygen luminescence kinetics in a heterogeneous environment – identification of the photosensitizer localization in small unilamellar vesicles†

S. Hackbarth and B. Röder

Received 24th June 2014,
Accepted 27th October 2014

DOI: 10.1039/c4pp00229f

www.rsc.org/pps

In vivo measurement of singlet oxygen luminescence kinetics is affected by the heterogeneity of biological samples. Even though singlet oxygen luminescence detection is technically getting easier, the analysis of signals from biological samples is still far from quantitative real time surveillance as it is aspired by the community. In this paper small unilamellar vesicles (SUVs) are used for modelling the general behaviour of heterogeneous samples. The geometry of the SUVs can be determined independently using dynamic light scattering. Therefore an accurate theoretical description of the generation, deactivation and diffusion of the singlet oxygen is possible. The theoretical model developed here perfectly fits the experimental results. Thus the location of the singlet oxygen generating a photosensitizer molecule can be exactly determined from the kinetics of the singlet oxygen luminescence. The application of the used theoretical approach thus allows for accurate quantitative measurements in SUVs.

1. Introduction

Singlet oxygen, the lowest electronically excited state of molecular oxygen may deactivate *via* weak, but characteristic luminescence around 1270 nm. For a long time the detection of this luminescence was quite difficult. The development of NIR-PMTs by Hamamatsu improved this situation and counting devices (multi scaler or time-correlated multi photon counting) became state of the art for such luminescence measurements as they are superior to classical analogue devices.[1] Measurements *in vitro* and *in vivo* became possible,[2–4] but the results obtained this way have already revealed that fitting based on the assumption of a homogeneous environment near the photosensitizer (PS) may not be sufficient to describe the observed luminescence kinetics.

In a homogeneous environment the kinetics of singlet oxygen concentration (c_Δ) after a delta pulse excitation at time $t = 0$ can be described as a double exponential curve, determined by the feeding at the speed of the photosensitizer (PS) triplet decay τ_T and quenching by the solvent and other quenchers therein. The natural lifetime of $^1O_2$ is way too long to have a significant influence on the kinetics in any solution. The tricky part is that the assignment of the involved decay times to signal increase and fall may switch. It is the faster of both times that determines the increase and the slower that determines the decay:

$$c_\Delta(t) = (c_{PS}(0)\Phi_\Delta {\tau_T}^{-1}/({\tau_T}^{-1} - {\tau_\Delta}^{-1}))(\exp(-t/\tau_\Delta) - \exp(-t/\tau_T)), \quad (1)$$

where $c_{PS}(0)$ describes the initial concentration of excited PS, Φ_Δ is the $^1O_2$ quantum yield and τ_Δ is the decay time of $^1O_2$.

In contrast to former assumptions that in heterogeneous environments the luminescence follows an average kinetics, if only the areas of the different phases were small compared to the diffusion length of $^1O_2$,[2,5] recent improvements of the sensitivity of $^1O_2$ luminescence detection proved that this is not the case.[6]

If the $^1O_2$ generating PSs are not homogeneously distributed over all phases of a heterogeneous environment and the radiative rate constant differs between the phases, then the diffusion of $^1O_2$ affects the signal kinetics. In a biological environment this effect is especially visible, if the $^1O_2$ is generated by membrane localized PSs. On the other hand the radiative rate constant in the membrane is much bigger compared to the surrounding aqueous environment.[7] On the other hand the diffusion length of $^1O_2$ in water is quite short. Based on the generally agreed value of the diffusion coefficient of oxygen in water $D = 2 \times 10^{-5}$ cm^2 s^{-1},[8,9] three dimensional

Humboldt-Universität zu Berlin, Institute of Physics, Photobiophysics, Newtonstr. 15, 12489 Berlin, Germany. E-mail: hacky@physik.hu-berlin.de, roeder@physik.hu-berlin.de

† Electronic supplementary information (ESI) available: Description of the mathematical formalism behind the spherical symmetrical diffusion model. See DOI: 10.1039/c4pp00229f

diffusion results in an average diffusion length of just around 200 nm. This value is based on the reported $^1O_2$ decay time in water of 3.7 ± 0.1 μs.[6] If just one dimensional diffusion applies, like in extended membranes (on the scale of $^1O_2$ diffusion this means just about a μm^2) the average diffusion length is about 120 nm. In comparison the thickness of a natural membrane of 4–12 nm[10,11] has to be taken into account. Therefore in the case of membrane localized PS a non-negligible signal can be registered from inside the membrane. This applies especially in case the radiative rate constant inside the membranes is bigger compared to water.[6] Diffusion of $^1O_2$ out of the membrane changes the temporal signal shape. Described vividly, the diffusion of $^1O_2$ out of the membrane (the area with a higher radiative rate constant) opens an additional decay channel for $^1O_2$ from inside the membrane. Any quantitative $^1O_2$ luminescence measurement in heterogeneous (*e.g.* biological) environments has to account for diffusion and different radiative rate constants. Here we report the first trial to do so. The scope of this paper is to demonstrate that for known membrane geometry evidence can be provided for such diffusion processes measuring the luminescence signal kinetics with high accuracy. Based on this knowledge it becomes possible to determine the localization of the PS relative to the membrane: whether it is in/at the lipid bilayer or not.

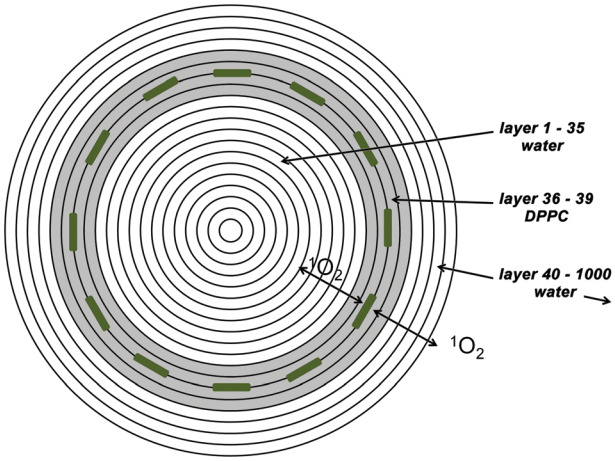

Fig. 1 The model for numerical simulations consists of concentric spherical shells (for better visibility the number of shells is reduced). The shells 36 to 39 (grey) represent the lipid bilayer where the PS are located. All other shells are assumed to be water. $^1O_2$ is generated in contact to the PS, thus in shells 37 and 38.

2. Materials and methods

The theoretical model

Liposomes were chosen as a model membrane system, since they are highly symmetric, having a defined thickness of the lipoid bilayer. Also their size can be determined *via* dynamic light scattering (DLS).

The diffusion of $^1O_2$ in this geometry can be described by a spherical symmetrical diffusion if the generation of $^1O_2$ (starting conditions) falls under this symmetry as well. The samples that will be analyzed in this paper are loaded with 50–100 PS molecules per liposome. Therefore the estimation of a spherical symmetrical PS distribution and singlet oxygen generation seems to be appropriate. Taking a liposome concentration where the distance between two liposomes is big compared to their size the model can be limited to a single liposome. The simulation therefore consists of 1000 concentric spherical layers of 1 nm thickness (Fig. 1), where layers 36 to 39 represent the liposomal membrane (according to the measured size of the SUVs using DLS – *vide infra*). The diffusion constant of oxygen in water at room temperature is reported to be 2×10^{-5} cm^2 s^{-1} and for membranes values in the literature are around 1×10^{-5} cm^2 s^{-1}.[5] These values are assigned to the layers accordingly as well as singlet oxygen decay times.

Recent calculations of the free energy for translocation of $^1O_2$ across a very similar bilayer (1-palmitoyl,2-oleoyl-*sn-glycero*-3-phosphocholine) report a higher solubility of $^1O_2$ inside the bilayer compared to the aqueous phase around.[12] This was also found experimentally for oxygen in another very similar bilayer (1,2-dimyristoyl-*sn-glycero*-3-phosphocholine) before.[13]

Similar partition coefficients (concentration ratio) of around 3.5 are reported in both papers and therefore the same value is used for our simulation.

If a PS is incorporated in a liposome membrane, it causes a certain deviation from the spherical shape, but since the model is spherically symmetric and thus diffusion only occurs radially the space occupied by the PS itself can be neglected. The volume increase of the layers with diameter is taken into account.

The numerical simulation for a given parameter set (PS triplet decay time and $^1O_2$ decay time outside the membrane) is carried out with time steps of 1.25×10^{-10} s. $^1O_2$ decay in the lipid bilayer is slow compared to the diffusion out of it and thus it has only minimal influence on the kinetics.[6] It is therefore set to 14 μs as reported for the DPPC films in ref. 2.

The overall $^1O_2$ amount in lipid layers and in water is calculated for the time interval 0–30 μs in steps of 20 ns.

The fit then is just an optimized linear combination of these two curves plus a constant background.

It is assumed that the singlet oxygen is generated in at least two layers with kinetics defined by the triplet decay time.

If a PS is really incorporated in the membrane the generation thus happens in layers 37 and 38, if the PS is attached to the membrane, the generation would happen in 4 layers: 34, 35, 39, and 40 as the oxygen can get the energy of the PS in the triplet state on both sides of the PS. In the case of water soluble PSs the singlet oxygen would be generated everywhere except in the membrane.

Due to the very fast diffusion between the layers and the small thickness of the membrane, the kinetics determined with this theoretical model are nearly indistinguishable for the PS embedded and attached to the layer. Just the amplitudes of the kinetics are minimally reduced for attached molecules,

about 6% for the lipid signal and 2% for the water signal. The SNR of singlet oxygen luminescence kinetics does not allow differentiation between these cases (not shown – after scaling they appear as one line).

Hydrodynamic diameter determined by dynamic light scattering (DLS)

The size of the prepared liposomes was determined using a commercial dynamic light scattering (DLS) setup Zetasizer Nano ZS (Malvern Instruments, UK) equipped with a He–Ne-Laser (wavelength = 632.8 nm) as described elsewhere.[14] The data were recorded at 25 ± 1 °C in backscattering mode at a 173° scattering angle. Each sample was measured three times for 100 s each measurement and the recorded data were averaged. Since the liposomes were filtered with a 0.22 μm syringe filter already, no further preparation was necessary. SUV concentrations were in the range of 10^{12}–10^{13} particles ml^{-1} which was reported to be a good value[15] for particles in this size range. Besides the average particle size the polydispersity index is determined during a DLS measurement. For a theoretical Gaussian size distribution it is the square of the normalized width at half height.

Time-resolved singlet oxygen luminescence kinetics

Luminescence kinetics were recorded using IF filter-based optics with central wavelengths at 1250, 1275 and 1300 nm. The collection times for the measurements at 1250 and 1300 nm were adjusted to compensate the different overall transmission of the filters. This means that any emission that has a more or less linear intensity distribution in this wavelength range causes the same signal intensity using the 1270 nm filter compared to the sum of the signals of the other two filters. So by subtracting the latter two signals from the first one results in a signal nearly free of distortion from scattering or PS phosphorescence if the maxima of these disturbing signals are sufficiently far away from this wavelength range.

Measurements were taken using the compact table-top $^1O_2$ luminescence detection system TCMPC1270 of SHB Analytics, Germany with the extension for using external lasers. Excitation was done using the frequency doubled Nd^{3+}-YAG Laser Vector from Coherent, Germany. Samples were excited with 5 mW at 532 nm, 10 ns pulses with a repetition rate of 12 kHz for 100 s when the 1270 nm filter was used.

The quality of each fit was ascertained using reduced χ^2 (χ^2_{red}) in the time region of 0.3–30 μs. The lower time limit was given by the ever present short time artifact.

$$\chi^2_{red} = \frac{\chi^2}{i_{max} - n}, \text{ with } \chi^2 = \sum_i \left(\frac{C_i - f(t_i)}{\sigma_i} \right)^2 \qquad (2)$$

where C_i represents the measured counts (difference of the three measurements – see above) for channel i, $f(t_i)$ is the theoretical value according to the fit function f. i_{max} is the number of channels and n represents the number of fit parameters. Since we are discussing about counting measurements with high count numbers the results follow Gaussian statistics and so Gaussian error propagation applies. The expected accuracy of each channel σ_i is thus given by the square root of the sum of all counts in the three measurements for this channel.

Triplet decay times

Flash photolysis measurements were taken using a ns-Nd^{3+}-YAG pumped OPO (Ekspla, 420–2500 nm). Transient triplet–triplet absorption was observed, perpendicular to the excitation, using a stabilized LED (λ_{max} = 488 nm), a band pass interference filter (488 nm) and a Si-photodiode with an integrated fast differential pre-amplifier (Elektronik Manufaktur Mahlsdorf, Germany). The setup allows the determination of triplet decay times down to 0.1 μs using a recording oscilloscope (HP5415).

Liposome preparation

Liposomes were prepared using the injection method described in ref. 16. Before injecting the ethanol solution of DPPC the PSs were mixed with the lipid molecules to ensure a homogeneous distribution. The concentration of the PS in the mixture before injection was about 0.1 mM. 1,2-Dipalmitoyl-*rac-glycero*-3-phosphocholine hydrate (DPPC) from Sigma-Aldrich, Germany was used as purchased. Directly after preparation, the liposomal solution was filtered through a 0.22 μm syringe filter. DLS measurements and detection of singlet oxygen kinetics as well as flash photolysis were done within a time frame of 6 hours after preparation. All measurements were taken at room temperature.

Photosensitizers

Pheophorbide a (Pheo) from Frontier Scientific, USA and *meso*-tetra(4-*N*-methyl-pyridyl) porphyrin (TMPyP) from Sigma-Aldrich, Germany were used as purchased.

In a previous study we used Pheo extracted from *Urtica urens*.[6,7] Analysing the purity of the extract using molecular mass spectrometry, besides Pheo with 593 Da, small amounts of pyro-Pheo have been identified with 535 Da. Since pyro-Pheo has a slightly longer triplet decay time compared to Pheo, even small contaminations disturb the analytic approach developed in this paper.

Because of that, for the actual investigation we used a commercial batch of Pheo. Its purity was checked using an Acquity-UPLC®-System equipped with a LCT Premier XE ESI-ToF mass spectrometer (positive mode). UPLC parameters: Acquity UPLC® BEH C18 column, 0.6 ml min^{-1}, 35 °C, solvent: 0.1% formic acid and acetonitrile in water, with a concentration gradient of acetonitrile from 60% to 95% within 10 minutes.

The sample we bought from Frontier Scientific did not contain other Pheo derivatives as *e.g.* pyro-pheophorbide according to this test and was therefore used for the experiments reported here.

3. Results and discussion

Pheo is well known to be incorporated in membranes due to its hydrophobicity[17] while TMPyP has very good water solubility[3] and thus it is a good reference for PSs equally distributed all over the water phase. Because of this these two PSs were chosen to test the applicability of the new diffusion model in competition to the standard two-exponential decay model imaging whether the luminescence kinetics reflect their localization relative to the SUVs.

The size of the SUVs formed after injection of DPPC mixed with Pheo as determined by DLS was astonishingly reproducible with a diameter of about 78 nm and a narrow particle distribution index (0.17–0.18). The SUVs formed in the presence of TMPyP also had a narrow distribution index (0.19–0.20) in each case but the average size was in the range 70–100 nm for different trials. However, this did not influence the results of the measured kinetics, as expected.

For TMPyP the results of flash photolysis and $^1O_2$ luminescence are shown in Fig. 2. The PS triplet decay was fitted as 1.89 ± 0.20 μs assuming a mono exponential decay of the transient triplet absorption. A standard two-exponential fit of the singlet oxygen kinetics results in 1.85 ± 0.10 μs and 3.76 ± 0.10 μs. The PS triplet decay times determined with both methods match perfectly and the $^1O_2$ decay time is just slightly longer than reported before for water but within the error range. χ^2_{red} for this fit is 0.99, which indicates a perfect fit. From the results it seems obvious that the vast majority of TMPyP is solved in the water phase of the liposomal dispersions. This result is not surprising, but it stands as a good reference for the samples with Pheo.

As mentioned above, Pheo is known to be incorporated in membranes.[17]

In liposomal dispersion we determined a Pheo triplet decay time of 1.98 ± 0.20 μs (Fig. 3, bottom) which is comparable to values reported before.[6]

In trying to fit the singlet oxygen luminescence decay curves using the standard two exponential fit, we obtained decay times of 1.5 μs and 4.2 μs. Neither does the triplet decay

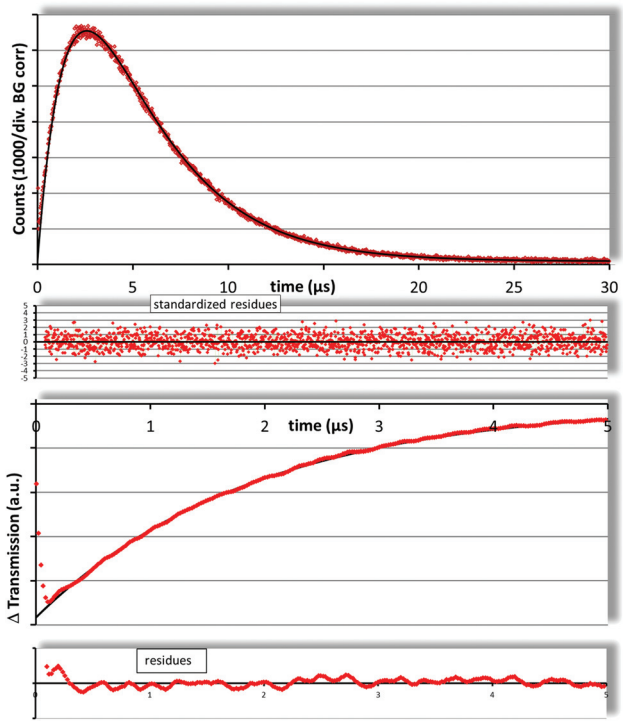

Fig. 2 The $^1O_2$ kinetics of SUVs with TMPyP (top) can be fitted using the standard two exponential description for homogeneous samples with decay times of 1.85 ± 0.10 μs and 3.76 ± 0.10 μs, which match the determined (flash photolysis – bottom) triplet decay of 1.89 ± 0.20 μs and the known $^1O_2$ decay in water (3.7 ± 0.1 μs).

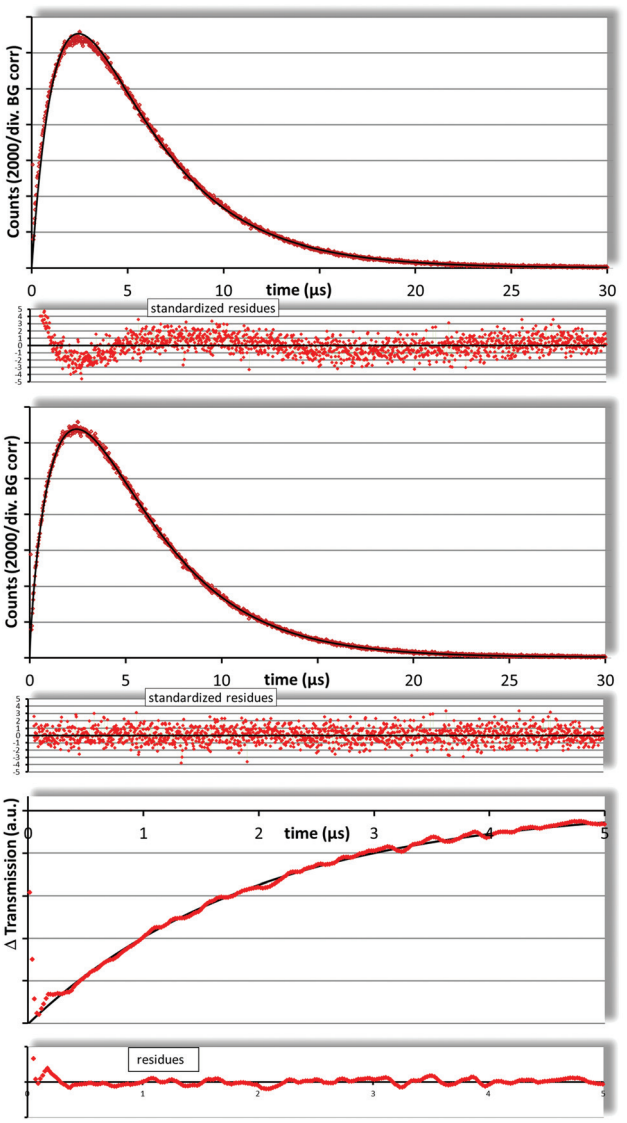

Fig. 3 Fitting the $^1O_2$ kinetics of SUVs with Pheo with the standard two exponential model (top) results in decay times that do not match the determined (flash photolysis – bottom) triplet decay time of 1.98 ± 0.20 μs. Also the residues are not at all symmetrically distributed. The fit using the new diffusion model (middle) results in 2.04 ± 0.10 μs and 3.84 ± 0.10 μs with much better residues.

time coincide with the one determined by flash photolysis nor is the $^1O_2$ decay time even near to the one in water. Due to the preparation of the liposomes with the injection method there is about 5–7% ethanol in the solution, but in test measurements of water–ethanol mixtures we found that it would require more than 30% ethanol in the solution to raise the $^1O_2$ decay time above 4 μs (not shown). It has been reported that ethanol concentrates in the vicinity of the membranes but this effect is limited to the lipid water interface and consequently not that strong.

Finally, a look at the residua of the fit reveals that this fit does not describe the measured kinetics (Fig. 3, top).

Obviously, the commonly used two exponential model is not an appropriate description of the kinetics of $^1O_2$ photosensitivity generated by Pheo in liposome dispersions. This proves that the $^1O_2$ is not generated equally distributed within the sample, a fact that is known, but here for the first time can be directly derived from $^1O_2$ kinetics.

The results shall now be fitted based on the above described model of singlet oxygen generation only in the membrane bilayer followed by diffusion.

The fitting procedure: the PS triplet (1 μs⋯3 μs) and the singlet oxygen decay time outside the membrane (3 μs⋯5 μs) is stepwise varied in steps of 0.02 μs and for each parameter set the theoretical temporal development of the amount of $^1O_2$ inside and outside the membrane is calculated. These calculations are based on Fick's laws of diffusion (see ESI†). The fit is then a linear combination of the two curves plus a constant background since the dark counts of the device are equally distributed over time. The ratio of the amplitudes of the two curves is also the ratio of the radiative rate constants in the membrane compared to the aqueous solution around it (rate ratio). It is known that the radiative rate constant of $^1O_2$ depends on the environment.[18]

The best fit was obtained for a PS triplet decay time of 2.04 μs, a $^1O_2$ decay time of 3.84 μs and an rate ratio of 3.25 (Fig. 3, middle). The corresponding value for χ^2_{red} is 1.07 (time region 0.3–30 μs). In Fig. 4 the best obtained χ^2_{red} are shown as a function of the parameter set. The central white area represents values below 1.1, the grey area around it goes up to 1.2 and so on. The large white field means $\chi^2_{red} > 2.9$ and is therefore of no interest. The black lines across this plot connect the parameter sets that result in the same rate ratio. From the left to the right the lines represent rate ratios from 2 to 4.5 in steps of 0.5. The region of best fits ($\chi^2_{red} < 1.1$) includes rate ratios from 2.9 to 3.7, so we can assume a value of 3.25 ± 0.50. This value is much smaller than the one reported earlier.[6] This is mainly due a more accurate model (spherical symmetrical instead of 1D diffusion/solubility of $^1O_2$ is taken into account, which was not performed in the past) and Pheo of a higher purity (see section 2).

The PS triplet decay time determined by our model perfectly corresponds to the result of the flash photolysis (Fig. 3, bottom) and the singlet oxygen decay time is only very slightly longer than it should be expected for the given content of ethanol in the solutions, which probably can be explained by the already mentioned affinity of ethanol to the lipid water interface.

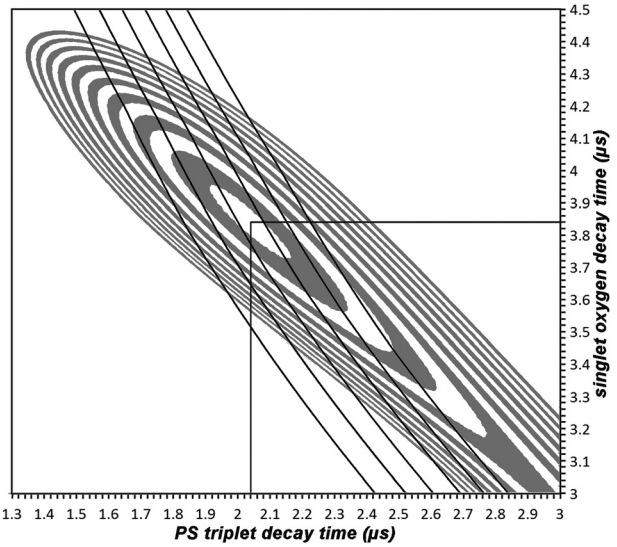

Fig. 4 Fit quality (reduced chi^2) of the diffusion model as a function of the parameter set (PS triplet, $^1O_2$ decay outside the membrane). The inner white area represents values up to 1.1, the dark area around goes up to 1.2 and so on. The outer white area means 2.9 or higher. The black lines across the diagram connect parameter sets which have a best fit for the same rate ratio. The lines represent the values 2 to 4.5 in steps of 0.5 (left to right).

4. Conclusions

It could be clearly shown that diffusion of $^1O_2$ influences its luminescence kinetics in heterogeneous systems. The temporal shape of the $^1O_2$ luminescence in the heterogeneous environment is not just an average of the involved phases, but depends strongly on the exact place of $^1O_2$ generation and the radiative rate constants of $^1O_2$ in different phases. For DPPC liposomes the $^1O_2$ luminescence emanating from inside the lipid bilayer is overpronounced by a rate ratio of 3.25 ± 0.50 compared to the surrounding water. Moreover, by analyzing the $^1O_2$ luminescence kinetics it was shown that Pheo in the liposomes generates $^1O_2$ in or in close vicinity to the membrane bilayer. On the other hand, TMPyP is nearly homogeneously distributed in the aqueous phase of the liposome dispersion and generates $^1O_2$ accordingly, whereby the luminescence kinetics can be described using the two exponential standard model.

Knowledge about such diffusion effects and different rate ratios of $^1O_2$ in biologically relevant environments will help to develop means for measuring $^1O_2$ directly and quantitatively *in vivo*.

Acknowledgements

The authors like to thank Matthias Girod from BAM – Federal Institute for Materials Research and Testing, Berlin, Germany

for his fast and kind help. He carried out the DLS measurements for us. Thanks to Sebastian Wieczorrek from the Chemical Department of Humboldt University. He checked the purity of the used Pheo with mass spectrometry. The authors gratefully acknowledge the inspirations given by the reviewers.

Notes and references

1 A. Jiménez-Banzo, X. Ragàs, P. Kapusta and S. Nonell, Time-resolved methods in biophysics. 7. Photon counting vs. analog time-resolved singlet oxygen phosphorescence detection, *Photochem. Photobiol. Sci.*, 2008, **7**(9), 1003.

2 T. Maisch, J. Baier, B. Franz, M. Maier, M. Landthaler, R.-M. Szeimies and W. Baumler, The role of singlet oxygen and oxygen concentration in photodynamic inactivation of bacteria, *Proc. Natl. Acad. Sci. U. S. A.*, 2007, **104**(17), 7223–7228.

3 M. K. Kuimova, S. W. Botchway, A. W. Parker, M. Balaz, H. A. Collins, H. L. Anderson, K. Suhling and P. R. Ogilby, Imaging intracellular viscosity of a single cell during photoinduced cell death, *Nat. Chem.*, 2009, **1**(1), 69–73.

4 M. T. Jarvi, M. J. Niedre, M. S. Patterson and B. C. Wilson, The Influence of Oxygen Depletion and Photosensitizer Triplet-state Dynamics During Photodynamic Therapy on Accurate Singlet Oxygen Luminescence Monitoring and Analysis of Treatment Dose Response, *Photochem. Photobiol.*, 2011, **87**(1), 223–234.

5 J. Baier, M. Maier, R. Engl, M. Landthaler and W. Bäumler, Time-Resolved Investigations of Singlet Oxygen Luminescence in Water, in Phosphatidylcholine, and in Aqueous Suspensions of Phosphatidylcholine or HT29 Cells, *J. Phys. Chem. B*, 2005, **109**(7), 3041–3046.

6 S. Hackbarth, J. Schlothauer, A. Preuß and B. Röder, New insights to primary photodynamic effects – Singlet oxygen kinetics in living cells, *J. Photochem. Photobiol., B: Biol.*, 2010, **98**(3), 173–179.

7 S. Hackbarth, J. Schlothauer, A. Preuß, C. Ludwig and B. Röder, Time resolved sub-cellular singlet oxygen detection – ensemble measurements versus single cell experiments, *Laser Phys. Lett.*, 2012, **9**(6), 474–480.

8 F. C. Tse and O. C. Sandall, Diffusion Coefficients for Oxygen and Carbon Dioxide in Water at 25 °C by Unsteady State Desorption from a Quiescent Liquid, *Chem. Eng. Commun.*, 1979, **3**(3), 147–153.

9 M. Jamnongwong, K. Loubiere, N. Dietrich and G. Hébrard, Experimental study of oxygen diffusion coefficients in clean water containing salt, glucose or surfactant: Consequences on the liquid-side mass transfer coefficients, *Chem. Eng. J.*, 2010, **165**(3), 758–768.

10 R. A. Freitas, Jr., *Nanomedicine, Volume I: Basic Capabilities*, Landes Bioscience, Georgetown (Tex.), 1999.

11 K. Mitra, I. Ubarretxena-Belandia, T. Taguchi, G. Warren and D. M. Engelman, Modulation of the bilayer thickness of exocytic pathway membranes by membrane proteins rather than cholesterol, *Proc. Natl. Acad. Sci. U. S. A.*, 2004, **101**(12), 4083–4088.

12 R. M. Cordeiro, Reactive oxygen species at phospholipid bilayers: distribution, mobility and permeation, *Biochim. Biophys. Acta*, 2014, **1838**(1 Pt B), 438–444.

13 E. Smotkin, F. T. Moy and W. Plachy, Dioxygen solubility in aqueous phosphatidylcholine dispersions, *Biochim. Biophys. Acta, Biomemb.*, 1991, **1061**, 33–38.

14 L. Böhmert, M. Girod, U. Hansen, R. Maul, P. Knappe, B. Niemann, S. M. Weidner, A. F. Thünemann and A. Lampen, Analytically monitored digestion of silver nanoparticles and their toxicity on human intestinal cells, *Nanotoxicology*, 2014, **8**(6), 631–642.

15 J. Panchal, J. Kotarek, E. Marszal and E. M. Topp, Analyzing Subvisible Particles in Protein Drug Products: a Comparison of Dynamic Light Scattering (DLS) and Resonant Mass Measurement (RMM), *AAPS J.*, 2014, **16**(3), 440–451.

16 A. Zeug, A. Paul and B. Röder, Observation of the phase transition in phospholipid liposomes taking advantage of the particular optical properties of octa-α-butyloxy-H 2 phthalocyanines, *J. Porphyrins Phthalocyanines*, 2001, **05** (09), 663–667.

17 B. Röder, T. Hanke, S. Oelckers, S. Hackbarth and C. Symietz, Photophysical properties of pheophorbide a in solution and in model membrane systems, *J. Porphyrins Phthalocyanines*, 2000, **4**(1), 37–44.

18 T. D. Poulsen, P. R. Ogilby and K. V. Mikkelsen, Solvent Effects on the O 2 (a 1 Δ g)–O 2 (X 3 Σ g-) Radiative Transition: Comments Regarding Charge-Transfer Interactions, *J. Phys. Chem. A*, 1998, **102**(48), 9829–9832.

